International Journal of Multiphase Flow 58 (2014) 39–51

Contents lists available at ScienceDirect

International Journal of Multiphase Flow

journal homepage: www.elsevier.com/locate/ijmulflow

Optimization of capillary flow through square micropillar arrays

R.S. Hale [a], R.T. Bonnecaze [b], C.H. Hidrovo [a,*]

[a] Multiscale Thermal Fluids Laboratory, Department of Mechanical Engineering, The University of Texas, Austin, TX, USA
[b] Department of Chemical Engineering, The University of Texas, Austin, TX, USA

ARTICLE INFO

Article history:
Received 18 September 2012
Received in revised form 13 August 2013
Accepted 14 August 2013
Available online 28 August 2013

Keywords:
Capillary flow
Wicking
Micropillar
Permeability
Heat pipe

ABSTRACT

This work compares several models for fluid flow through micropillar arrays to numerical simulations and uses them to optimize pillar dimensions for maximum fluid flow in a heat pipe application. Micropillar arrays are important for controlling capillary flow in microfluidic devices, and array permeability is a key parameter in determining fluid flow rate. Several permeability models are considered, including the Brinkman equation, numerical simulations, inverse reciprocal sums of a cylinder bank and open flow over a flat plate, and an analytical solution developed by the authors derived from a 2-dimensional velocity profile with appropriately varying boundary conditions. The comparison seeks to identify the models that are reliable over a wide range of porosities yet flexible enough to accommodate new pillar configurations. Numerical simulations of pillar permeability are the most desirable due to their accuracy. For pillars arranged in a square pattern, the 2-D analytical solution proposed in this study performs well at short pillar heights while the Brinkman equation is more accurate at tall pillar heights. Therefore, a hybrid model is formulated that uses the 2-D solution for $h/d \leqslant 5$ and the Brinkman model for $h/d > 5$. The 2-D solution, the Brinkman equation using specifically the permeability derived by Tamayol and Bahrami (2009), and numerical simulations are easily adapted to alternative pillar arrangements. A comparison of these models for pillars arranged in a rectangular pattern demonstrated that the authors' proposed solution is an excellent match to numerical results. These findings are applied to capillary fluid flow in heat pipes to explore the effects of pillar spacing, diameter, and height on the maximum fluid flow rate through the wick. At a given height aspect ratio, there is an optimum pillar spacing that balances the viscous losses and driving capillary pressure such that the flow rate reaches a maximum. In addition, the flow rate is increased by increasing pillar height if the pillar spacing is maintained at the corresponding optimum point.

1. Introduction

Microscale pillar arrays have received extensive attention due to their applicability to a wide range of technologies. Lab-on-a-chip systems have used pillar arrays for high-performance liquid chromatography (de Beeck et al., 2012; Song et al., 2012), dielectrophoresis (Cui and Lim, 2009), and isolating cancer cells (Nagrath et al., 2007; Sheng et al., 2012). Thermal management is another area of interest, where pillars have recently been studied for use in a flat plate heat pipe (Lips et al., 2010; Nam et al., 2010; Lefevre et al., 2012). One of the key parameters of interest for these technologies is the macroscopic rate of fluid flow through the array. The flow rate is dictated by the balance of the permeability and capillary forces of the pillar array. Small pore radii result in large driving capillary pressures but decrease permeabilities. Therefore, the ability to accurately predict the permeabilities of pillar arrays is crucial to their design and utilization.

Sangani and Acrivos (1982) studied the viscous permeability of square and hexagonal cylinder arrays at high and low porosity limits. Drummond and Tahir (1984) modeled flow around long fibers using a cell approach to find permeabilities at high porosities. Gebart (1992) used the lubrication approximation for transverse flow through square and hexagonal cylinder arrays to find an expression for the permeability at low porosities. Yazdchi et al. (2011) compiled a summary of cylinder array permeability models and compared them to finite element simulations, then created a hybrid equation valid for all porosities based on Gebart (1992) and Drummond and Tahir (1984). Yazdchi et al. (2012) later extended the finite element simulations to investigate random cylinder arrays. Tamayol and Bahrami (2009) and Zhang et al. (2010) used cell approaches to model actual pillar arrays as opposed to long cylinder arrays. Xiao and Wang (2011) and Byon and Kim (2011) used the Brinkman equation for flow through porous media to find an analytical solution for permeability. Tamayol et al. (2013) calculated the pressure drop for flow through

* Corresponding author. Tel.: +1 5122320865.
E-mail address: hidrovo@mail.utexas.edu (C.H. Hidrovo).
URL: http://www.me.utexas.edu/~hidrovo (C.H. Hidrovo).

0301-9322/$ - see front matter © 2013 Elsevier Ltd. All rights reserved.
http://dx.doi.org/10.1016/j.ijmultiphaseflow.2013.08.003

a microchannel filled with a pillar array. Their method used the Brinkman equation and resulted in a hyperbolic solution. Finally, Srivastava et al. (2010) used numerical simulations to develop a predictive equation for the volumetric flow rate of liquid through a limited range of pillar geometries, and Ranjan et al. (2012) used numerical simulations to develop correlations for pillar array permeability as a function of porosity for different pillar shapes.

These models have yet to be compared side-by-side. Srivastava et al. (2010), Ranjan et al. (2012), and Yazdchi et al. (2011) demonstrated the use of state-of-the-art numerical simulations which give exact predictions of pillar systems. In addition, the models of cylinder banks by Gebart (1992), Drummond and Tahir (1984), and Sangani and Acrivos (1982) are excellent analytical solutions for the porosity regimes in which they were developed. Alternatively, Tamayol and Bahrami (2009) and Zhang et al. (2010) proposed approximate analytical solutions which are more easily manipulated to reflect changes in pillar geometry. The design of micropillar wicks requires a robust model that applies to all porosities, yet is flexible enough to allow rapid testing of new ideas. This study seeks to identify such a model from the current approaches.

Since the permeability of a pillar array is solely a function of pillar geometry, researchers can customize flow rate predictions to their specific application with the capillary pressure drop. Some applications require fluid to move as a liquid propagation front, others as a continuous flow. Liquid front propagation technologies have pressure drops that relate to surface energies and dynamic meniscus shapes (Ishino et al., 2007; Xiao et al., 2010; Xiao and Wang, 2011). Continuous flow technologies have pressure drops that rely primarily on the effects of pillar geometry on meniscus shape (Peterson, 1994; Lips et al., 2010; Ranjan et al., 2012). Here we are interested in the particular application of flat plate heat pipes (FPHP) with microstructured wicks for thermal management.

Heat pipes are cooling devices that utilize passive capillary fluid flow through internal wicking structures to remove heat via a phase change process in a closed system. Wang and Bar-Cohen (2007) concentrated on the need for on-chip cooling technologies to combat hot spots on silicon chips. Therefore, small size and uncomplicated operation is desirable for electronic cooling. Micropillar arrays have the potential to contribute in this area, but the majority of recent modeling work has focused on liquid front propagation technologies. Lips et al. (2010) characterized the liquid–vapor interface of fluid flow through 2-D wicking structures in FPHP with confocal microscopy, and Lefevre et al. (2012) expanded the work to include meniscus curvature measurements along the length of the heat pipe. One of their wicking structures consisted of rectangular micropillars arranged in a square pattern. Sharratt et al. (2012) investigated the phase change heat transfer performance of copper micropillars arranged in several different geometric designs. We seek to optimize pillar array dimensions to achieve maximum fluid flow through a micropillar wick for heat pipe applications.

2. Fluid flow models

Imagine an array of pillars with diameter d, height h, edge-to-edge distance in the y-direction w, edge-to-edge distance in the x-direction s, and center-to-center distance in the x-direction $l = w + d$ (Fig. 1). For a square pattern, $w = s$. Fluid flow occurs in the x-direction, and the liquid interface at h is assumed to be flat. A few recent studies have included the effects of meniscus shape on permeability (Xiao et al., 2010; Xiao and Wang, 2011; Byon and Kim, 2011), but the interface was kept flat in this study to compare across a broader range of modeling work. This study will only consider an array unbounded by macroscopic sidewalls, but Vangelooven and Desmet (2010) have pointed out that the sidewalls of a bounded array must be carefully placed to avoid discrepancies between the bulk velocity and the edge velocity.

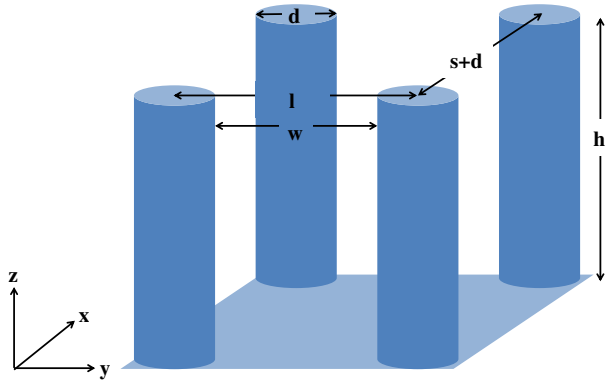

Fig. 1. Micropillar unit cell with geometric parameters. Fluid flow is in the x-direction.

If the pressure gradient is assumed to be constant and is applied only in the x-direction, the Darcy fluid flow model states that the superficial fluid velocity U is related to the pressure gradient across the system dP/dx such that

$$U = -\frac{dP}{dx}\frac{K}{\mu}, \tag{1}$$

where K is the sample permeability and μ is the fluid viscosity. The permeability is commonly non-dimensionalized by the pillar diameter, such that $K^* = K/d^2$. Thus, calculating the mass flow rate through a micropillar array requires knowledge of the dimensionless permeability.

2.1. Cylinder bank and flat plate combination

One approach to calculating the permeability through a micropillar array is to combine the permeability of an unbounded cylinder bank with the permeability of a flat plate by assuming a constant superficial velocity through the array and utilizing the fact that total pressure drop is equal to the sum of the individual component pressure drops:

$$U = -\left(\frac{dP_{cyl}}{dx}\right)\frac{K_{cyl}}{\mu} = -\left(\frac{dP_{plate}}{dx}\right)\frac{K_{plate}}{\mu} \tag{2}$$

$$\left(\frac{dP_{total}}{dx}\right) = \left(\frac{dP_{cyl}}{dx}\right) + \left(\frac{dP_{plate}}{dx}\right). \tag{3}$$

Solving Eq. (2) and (3) simultaneously gives

$$K^*_{total} = \left(\frac{1}{K^*_{cyl}} + \frac{1}{K^*_{plate}}\right)^{-1}, \tag{4}$$

which weights each individual permeability such that the total permeability automatically reflects the dominance of either the flat plate or cylinder bank characteristics of the array. The permeability of a flat plate is derived from steady, laminar flow driven by a constant pressure gradient and having no-slip and free surface boundary conditions at $z = 0$ and $z = h$, respectively (Deen, 1998):

$$K_{plate} = \frac{1}{3}h^2\epsilon. \tag{5}$$

The 2-dimensional porosity, ϵ (Eq. (6)), accounts for the fact that Eq. (1) refers to superficial velocity.

$$\epsilon = 1 - \frac{\pi}{4}\frac{d^2}{l^2}. \tag{6}$$

Since d is the parameter chosen for non-dimensionalization, Eq. (7) gives the final result for K^*_{plate} even though d does not have a direct physical meaning for a plate without pillars.